Engineering Research Express

PAPER

A simple and low-cost approach for the synthesis and fabrication of ZnO nanosheet-based nanogenerator for energy harvesting and sensing

To cite this article: P Supraja *et al* 2021 *Eng. Res. Express* **3** 035022

Engineering Research Express

PAPER

A simple and low-cost approach for the synthesis and fabrication of ZnO nanosheet-based nanogenerator for energy harvesting and sensing

RECEIVED
14 June 2021

REVISED
30 June 2021

ACCEPTED FOR PUBLICATION
27 July 2021

PUBLISHED
6 August 2021

P Supraja[1], Rakesh Kumar R[1], Siju Mishra[1], D Haranath[1], P Ravi Sankar[2] and K Prakash[2]

[1] Department Of Physics, Energy Materials and Devices Lab, National Institute of Technology-Warangal, Telangana, 506004, India
[2] Department Of Electronics Communication and Engineering, Flexible Electronics Lab, National Institute of Technology-Warangal, Telangana, 506004, India

E-mail: rakeshr@nitw.ac.in

Keywords: piezoelectric materials, energy storage and conversion, hydrothermal synthesis, energy harvesting, nanogenerator, sensing application

Supplementary material for this article is available online

Abstract

Reducing the cost of the synthesis process and device fabrication plays an essential role in modestly developing products. In the present report, a simple and low-cost approach for the synthesis of ZnO nanosheets and the fabrication of a piezoelectric nanogenerator is developed. The ZnO nanosheets are synthesized by hot plate assisted hydrothermal method and characterized for their morphology, crystallinity, composition. The fabricated nanogenerator device produced an open-circuit voltage of ~220 mV upon finger tapping. The series connection of seven such devices produced an open-circuit voltage of ~1.2 V. The ZnO nanosheets films synthesized at a growth temperature of 85 °C for a growth duration of 4 h are found to be optimum parameters for making the nanogenerator device with high output. The nanogenerator response is recorded for different frequencies of finger tapping and different finger-tapping pressures. Further, the fabricated nanogenerator exhibited a stable output response over 1100 cycles confirms the high durability of the fabricated device. The fabricated nanogenerator is explored further for pressure sensing application.

1. Introduction

Recently, most of the research focused on energy harvesting due to environmental issues, carbon emissions, and the limited availability of fossil fuels [1, 2]. To address these difficulties, a new research field known as 'nanogenerators' has emerged, which uses piezoelectric materials to harness mechanical energy [3–5]. The ease with which mechanical energy could be converted to electrical energy utilizing a well-known piezoelectric property makes it even more attractive and potential. The main advantages of mechanical energy are widely and easily available everywhere in nature at all times. Nanogenerators have been used as actuators, sensors, photodetectors, self-powered devices [6–9]. Among all piezoelectric materials, zinc oxide (ZnO) is selected in the current work to fabricate the nanogenerator. ZnO has several advantages viz. non-toxicity, environmental friendly, biocompatibility, and excellent optical and electrical properties [10, 11]. Synthesis of ZnO nanostructures is easy, established, and involves a simple process compared to all other materials synthesis. Among different synthesis methods, the hydrothermal synthesis of ZnO nanosheets is simple, inexpensive, single-step process, and low-temperature process [12, 13]. The obtained nanosheets exhibited high mechanical durability as well [14]. Hydrothermal synthesis is adapted in this report for the synthesis of ZnO nanosheets.

Hydrothermal synthesis of ZnO nanosheets is a well-established method, and it deals with synthesis at a temperature less than 100 °C using a hot air oven in most of the literature [15]. A hot plate was used in the current work instead of a hot air oven to provide growth temperature to the growth precursor solution. The cost of the process was reduced appreciably by adapting this methodology. To the best of our knowledge, the

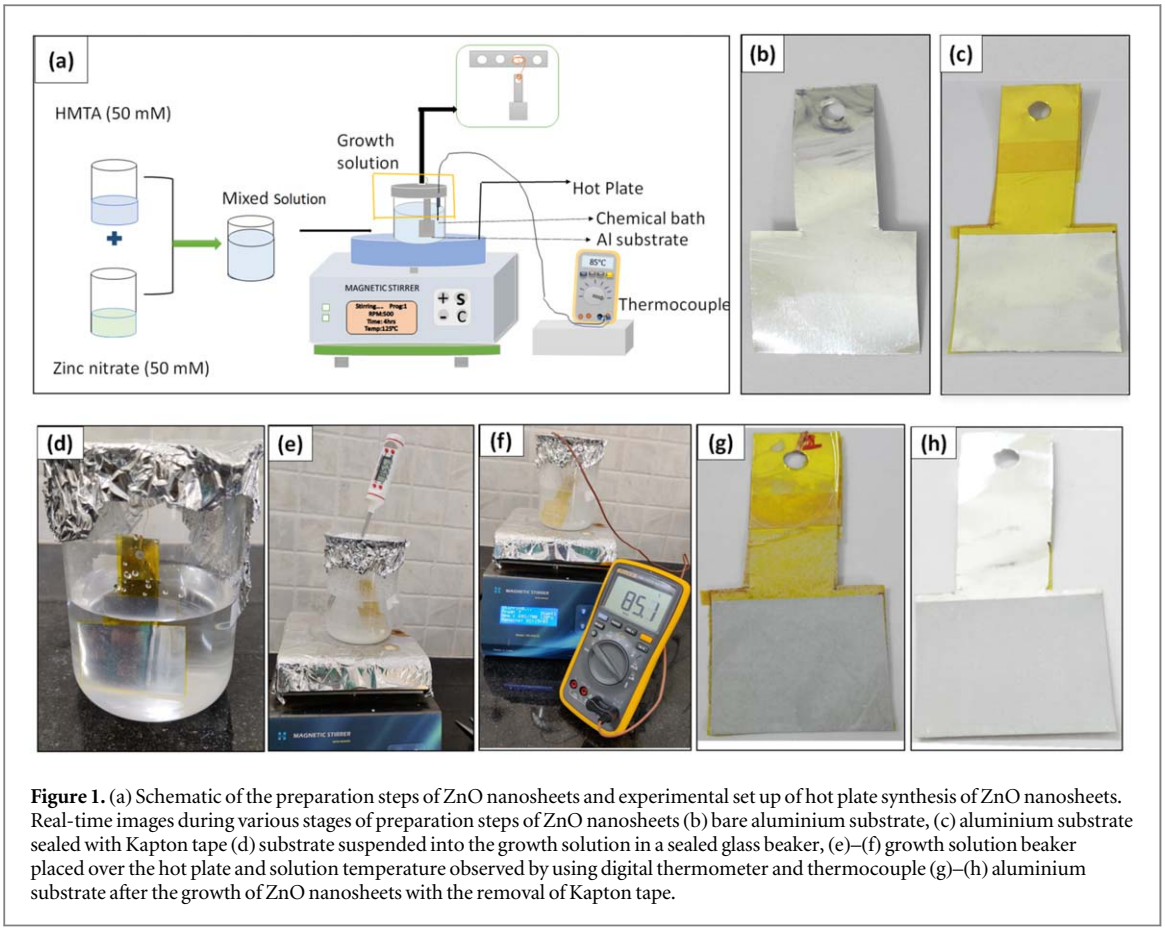

Figure 1. (a) Schematic of the preparation steps of ZnO nanosheets and experimental set up of hot plate synthesis of ZnO nanosheets. Real-time images during various stages of preparation steps of ZnO nanosheets (b) bare aluminium substrate, (c) aluminium substrate sealed with Kapton tape (d) substrate suspended into the growth solution in a sealed glass beaker, (e)–(f) growth solution beaker placed over the hot plate and solution temperature observed by using digital thermometer and thermocouple (g)–(h) aluminium substrate after the growth of ZnO nanosheets with the removal of Kapton tape.

synthesis of ZnO nanosheets using a hot plate has not been investigated so far, which forms the novelty of this paper. The novelty of the paper lies in the use of a low-cost hot plate for the ZnO nanosheets synthesis. It is a simple technique to synthesize nanostructures by directly heating of growth solution at the desired temperature. The hot plate-assisted hydrothermal method can be easily implemented for mass production of ZnO nanosheets films and larger area films for commercial applications. The main advantages of this new method are simple, low cost, rapid growth, catalyst-free, single-step synthesis.

In this work, we report a cost-effective and straightforward method to synthesize ZnO nanosheets using the hot plate-assisted hydrothermal method. Further nanogenerator was fabricated for mechanical energy harvesting and characterized for its electrical characteristics and sensing applications.

2. Experimental

2.1. ZnO nanosheets synthesis and characterization

The ZnO nanosheets film was synthesized on Al substrates using the hot plate method, as shown in the schematic diagram of figure 1(a). In the first instance, the aluminium substrates were ultrasonically cleaned with acetone and deionized (DI) water for 10 min, then dried under a hot-air blower. Initially, zinc nitrate ($Zn(NO)_3$. $6H_2o$, 50mM) and hexamethylenetetramine ($C_6H_{12}N_4$, HMTA, 50mM) were dissolved in 100ml of DI water and stirred for 10 min separately at room temperature. These two solutions were mixed in another beaker and stirred till the combined solution became transparent. One side of the aluminium substrate was sealed with Kapton tape and suspended in the growth solution, as shown in figures 1(b)–(c). The beaker containing the growth solution was covered with aluminium foil. A small opening was made to insert a thermocouple, as shown in figure 1 (d), for continuously monitoring the temperature. This small opening in the aluminium foil has been made such that it can be closed or opened depending on the requirement. Before performing synthesis, the growth precursor solution temperature was calibrated for 50 °C, 60 °C, 70 °C, 85 °C, 95 °C against applied hot plate temperature by inserting a thermocouple in the growth precursor solution. Finally, the beaker containing the growth precursor was kept over the hotplate at different growth temperatures for 4 h., ZnO-coated films on aluminium substrates were taken from the solution after 4 h of growth, rinsed with DI water, and dried with a hot-air blower.

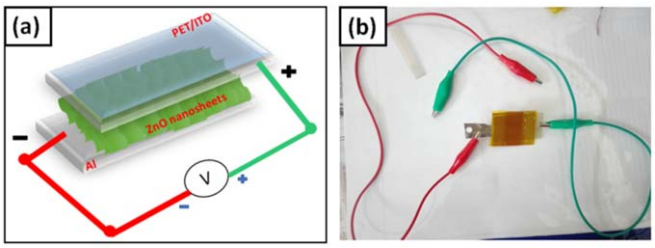

Figure 2. (a) Schematic of the device, (b) Actual image of the fabricated device.

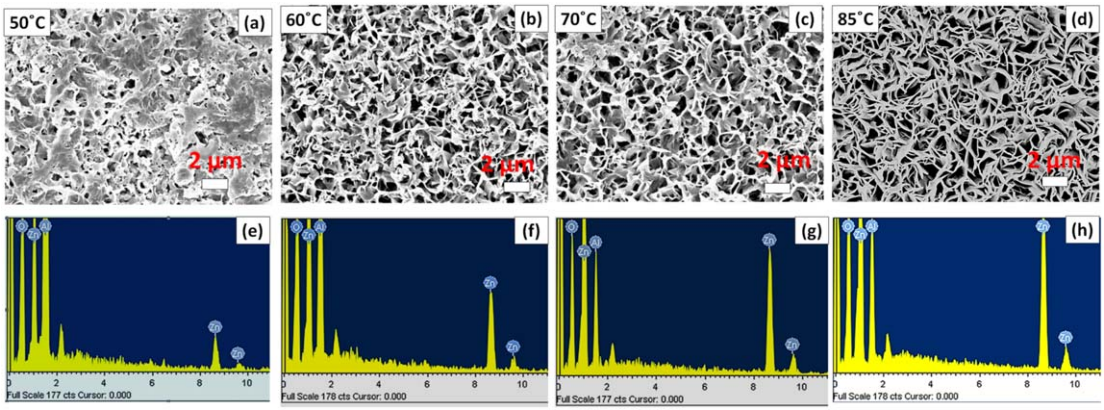

Figure 3. (a)–(d) Morphology of the ZnO films obtained at different temperatures, (e)–(h) EDS spectra of the ZnO nanosheet films.

Further, ZnO nanosheets growth was performed at different growth durations of 1, 2, 3, 4, 5, 6 h at a one selected optimum growth temperature of 85 °C. Several characterization techniques were performed to study the ZnO films. The ZnO films surface morphology and composition were analysed using a scanning electron microscopy (SEM, VEGA3 TESCAN) attached with energy dispersive spectroscopy (EDS). The crystallinity of the films was checked using by x-ray diffraction (XRD, Bruker D8) technique. The microstructure and crystallinity of the individual ZnO nanosheets were done using a transmission electron microscope (TEM, Tecnai G2 20).

2.2. Nanogenerator fabrication and testing

The fabrication of the nanogenerator required two conducting electrodes and piezoelectric nanostructure film. The schematic of the device fabrication is shown in figure 2(a). The uncoated region of aluminium foil shown in figure 1(h) is act as the bottom electrode, and ITO coated PET sheet acts as the top electrode. The ITO coated PET sheet was placed over the ZnO nanosheet film without making any short-circuit with a bottom aluminium electrode. This sandwiched (PET:ITO/ZnO nanosheets/Al) structure is sealed with Kapton tape rigidly to make proper contacts and avoid the triboelectric effect. Two conducting wires were connected to both the electrodes, as shown in figure 2(b).

The nanogenerator response against finger tapping was recorded using digital storage oscilloscope (Tektronix TBS1102) with the help of interfacing software (Tekvisa) to the computer. The response of the nanogenerator was recorded across different load resistances to find out the optimum power of the nanogenerator. Further, the response of the nanogenerator was also recorded for different finger-tapping pressures to apply the fabricated nanogenerator for practical pressure sensing applications.

3. Results and discussion:

Figures 3(a)–(d) shows the surface morphology of the ZnO thin films prepared at different growth temperatures of 50 °C, 60 °C, 70 °C, 85 °C, respectively. In all the cases, ZnO nanosheets are present all over the substrate except at 50 °C. These sheets are relatively vertically with respect to the substrate and also randomly distributed. Nanosheets are connected among them in a non-uniform way.

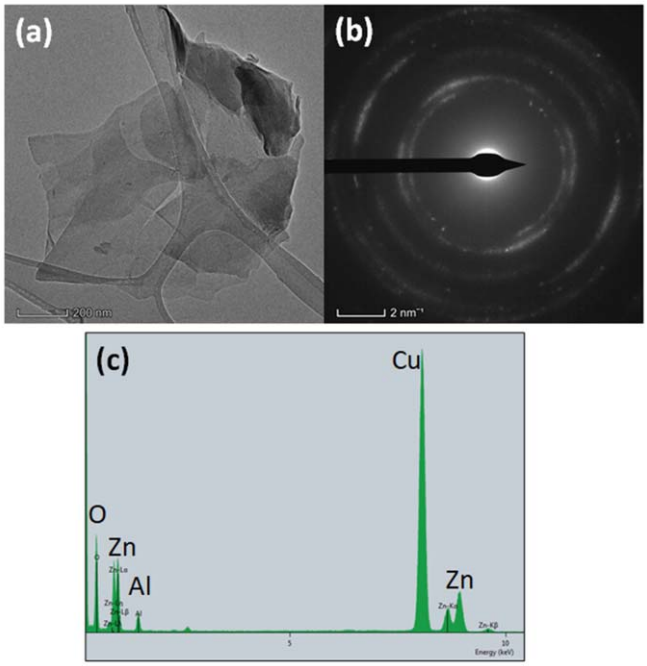

Figure 4. (a) TEM image of the ZnO nanosheet, (b) SAED pattern recorded on the ZnO nanosheets, (c) EDX spectrum recorded on the ZnO nanosheet.

The formation of the ZnO nanosheet is similar to the hydrothermal growth of ZnO nanosheets using a hot air oven [16]. Growth temperature plays a significant role in obtaining ZnO nanostructures. At lower temperatures of 50 °C and below, growth of nanosheets was not observed due to insufficient thermal energy for the decomposition of HMTA [16]. The uniform nanosheets growth was observed from 60 °C onwards and continued till 85 °C and above (See SI, S1 (available online at stacks.iop.org/ERX/3/035022/mmedia)). The differences observed in the morphology are due to the different densities and heights of the nanosheets, which in turn depends on the growth temperature. The growth rate of nanosheets increases with an increase in growth temperature as sufficient thermal energy is provided. Further, x-ray diffraction study confirms the polycrystalline nature of the ZnO nanosheet films (See SI, S2). Further, the purity of prepared films was studied by energy dispersive spectroscopy (EDS) and shown in figures 3(e)–(h). The EDS spectra of all the films show Zn, O, Al, and no other detected elements.

Figure 4(a) shows TEM image of the few nanosheets on the copper grid. The transparent nature of the nanosheets confirms the lesser thickness of the sample. Further, the selected area electron diffraction (SAED) pattern recorded on ZnO nanosheet exhibited the polycrystalline nature of the ZnO nanosheets. EDX spectrum recorded on the ZnO nanosheets further confirms the purity of the nanosheets.

The response of the nanogenerators fabricated from the ZnO nanosheet films synthesized at different growth temperatures is shown in figure 5(a). This response was recorded at uniform finger tapping pressure on the device under open-circuit conditions. It is clear from figures 5(a)–(b) that output voltage is increased with an increase in the growth temperature and saturated above 85 °C. The change in the output voltage can be correlated to ZnO nanosheet deformation's magnitude under applied pressure. At lower temperatures films, minor deformations can be expected due to sheet heights were small. At higher growth temperature films, large deformation can be expected due to significant sheet heights. The saturation in the output voltage at 85 °C and above may be due to the similar thickness of the nanosheet films. Therefore, a growth temperature of 85 °C is found to be the optimum growth temperature for higher nanogenerator output voltage. Further, the nanogenerator made up of ZnO nanosheet films synthesized at 85 °C were used for all other studies in the subsequent sections.

Figures 5(c)–(d) shows the typical response of the nanogenerators, which were fabricated with ZnO nanosheets films obtained at 85 °C for different growth durations of 1–6 h. Nanogenerator output is increasing with increasing growth duration and saturated for 4 h ZnO nanosheet films onwards. The ZnO nanosheets length increases with an increase of growth duration and saturates after a particular time. ZnO nanosheet length saturation with growth time due to consumption of all the OH^{-} ions and Zn^{+2} ions in the growth solution [17]. The saturation of ZnO nanosheets height was observed for 4 h of growth films and above. The height saturation of ZnO nanosheets results in the same deformation under applied pressure and produces the same output.

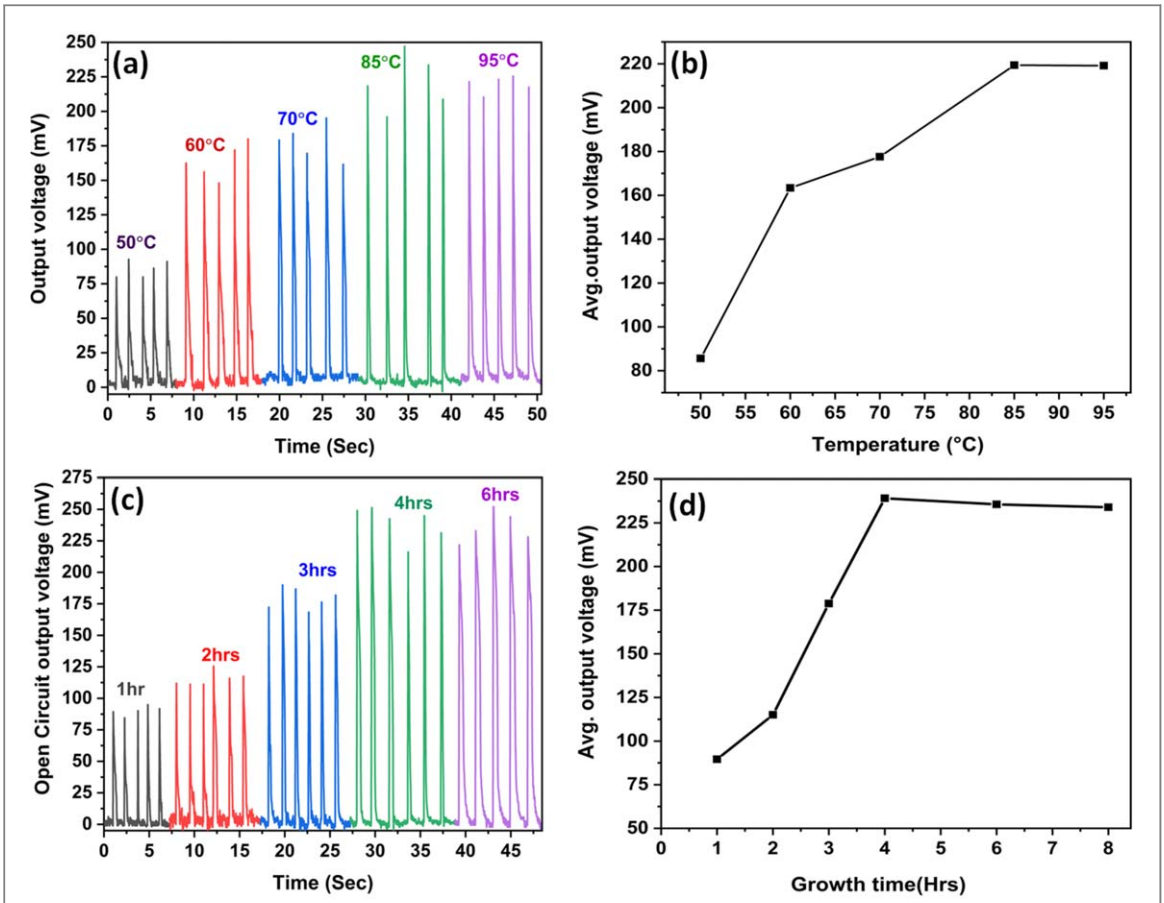

Figure 5. (a) Response of the nanogenerators fabricated with ZnO nanosheets films synthesized at different growth temperatures, (b) average output voltage of nanogenerators fabricated with ZnO nanosheets films synthesized at different growth temperatures, (c) response of the nanogenerators fabricated with ZnO nanosheets films synthesized at different growth durations, (d) average output voltage of nanogenerators fabricated with ZnO nanosheets films synthesized at different growth durations.

Figures 6(a)–(b) shows the response of nanogenerators under switching polarity test and linear superposition of voltage test. These tests were performed to confirm the output voltage generated from the nanogenerator alone, not by the oscilloscope or noise in the instrument [18–21]. In the switching polarity test: the forward and reverse connections were established by interchanging nanogenerator connections to the measuring device. The nanogenerator has shown exactly opposite voltage output signal in reverse connection with respect to the forward signal, as shown in figure 6(a) (See SI Video S1, S2). In both configurations, the output voltage of the nanogenerator is nearly the same. In the second test, the seven nanogenerator devices were connected in series to add up the voltages. The output voltages generated by the series-connected seven nanogenerators are shown in figure 6 (b), and an output voltage of ~1.2 V being measured (See SI Video S3, S4). These tests confirmed the output voltage generated from nanogenerator alone not by the oscilloscope or noise in the instrument.

Nanogenerator output voltage was recorded at different load resistances ranging from 10 KΩ to 100 MΩ under uniform hand tapping to measure the optimum output power. Figure 6(c) shows the variation of output voltage under different load resistances. With an increase in load resistance, the voltage increases and saturates at a value of approximately ~200 mV. The saturated output voltage at higher resistance (>10 MΩ) is close to the open circuit output voltage. Inset of the figure 6(c) shows the magnified view of output voltage up to 3 MΩ load resistance. The nanogenerator output voltage behaviour with load resistance can be understood with the help of a simple equivalent model proposed by Z L Wang and other research groups in the literature [22–25] (See SI, S3). Now, we can assume the nanogenerator device is equivalent to a voltage source, and load resistance (R_L) connected parallel to the device to measure voltage. The voltage drops across the R_L increase until the optimum R_L and saturate at the theoretically infinite load resistance similar to open-circuit voltage [26]. The load resistance dependence of output voltage shows a similar trend as reported in the literature for piezoelectric nanogenerators made of different materials [26–30].

The output power $\left(Power = \frac{V^2}{(R_L)}\right)$ of the nanogenerator with different load resistances was calculated and depicted in figure 6(d). The maximum output power of 65 nW was observed for the nanogenerator at 100 KΩ of

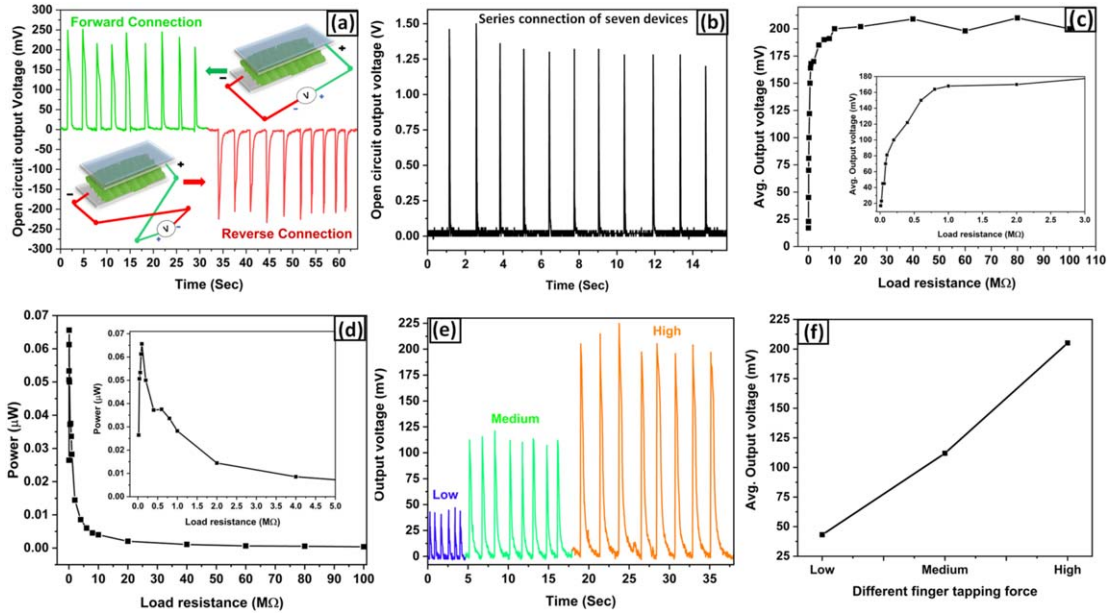

Figure 6. Nanogenerator output characteristics against finger tapping (a) forward and reverse connection response, (b) output voltage of the series-connected seven nanogenerators, (c) average output voltage of the nanogenerator across different load resistances, (d) the output power variation with variable load resistance, (e) response of the nanogenerator against different finger-tapping pressures, (f) average output voltage of the nanogenerator as a function of different finger-tapping pressures.

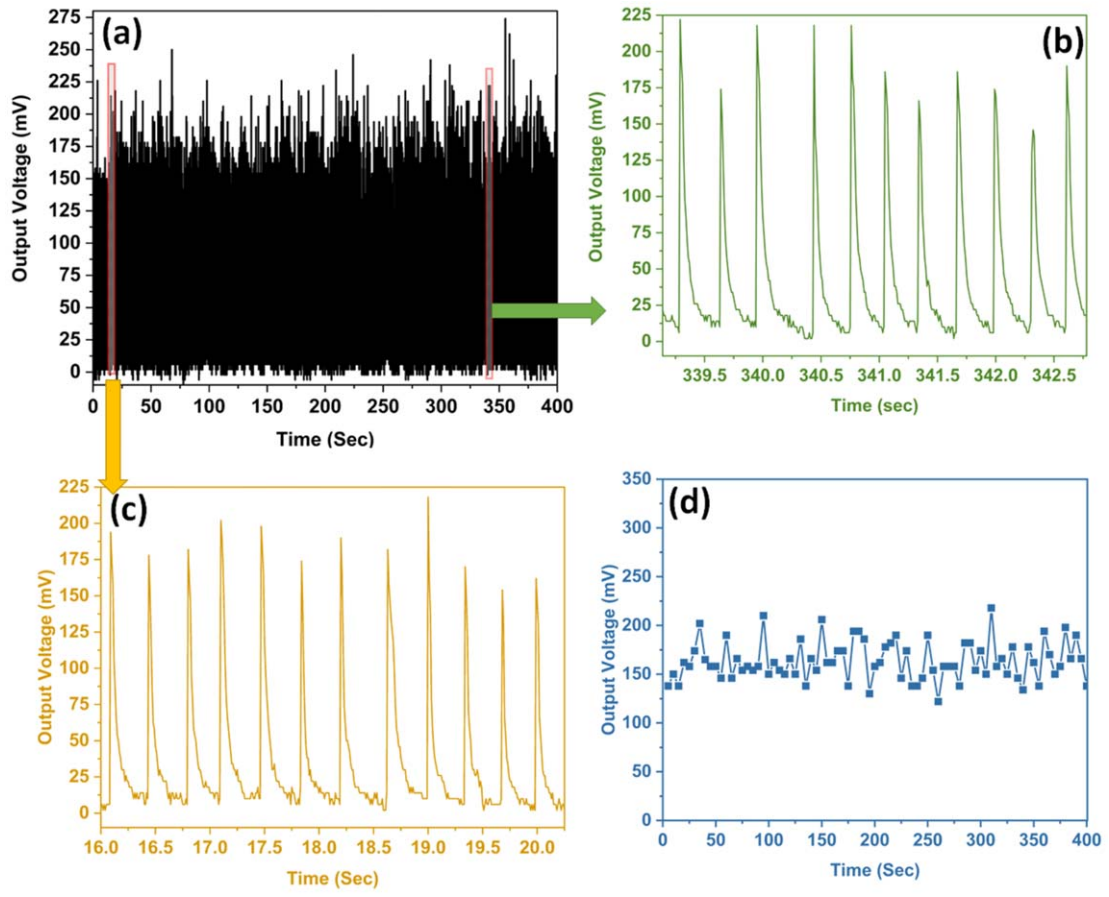

Figure 7. (a) nanogenerator response over 1100 cycles of finger tapping, (b)–(c) Magnified view of the selected region of the cycle test, (d) nanogenerator output at different cycle numbers.

load resistance R_L. Inset of the figure 3(d) shows the magnified view of output power up to 5 MΩ load resistance. The output power characteristics of the nanogenerator can be understood from the maximum power transmission theorem [31]. It states that maximum power transmission occurs when the load resistance value equals the source internal resistance. In the present report, the peak in output power occurred under impendence matched conditions across a load resistor value ∼100 KΩ. The output power decreased with the load resistance values greater than 100 KΩ due to the saturated output voltage. The saturated output voltage at higher load resistance decreases the V^2/R_L ratio (power) value. The dependence of output power with load resistance shows a similar trend as reported in the literature for piezoelectric nanogenerators made of different materials [32–34].

Further nanogenerator was explored for pressure sensing application. Figures 6(e)–(f) shows the response of the nanogenerator under different finger-tapping pressures of a low, medium, and high. The measured voltages are ∼40mV,110mV, and 200 mV for low, medium, and high tapping pressures. The amount of deformation in ZnO nanosheets rises as the pressure acting on the nanosheet increases, resulting in an increase in output voltage.

Further, the response of the nanogenerator tested over 1100 cycles is shown in figure 7(a). Figures 7(c)–(d) shows the magnified view of the nanogenerator response of figure 7(a). Further, the nanogenerator output voltage at different cycle numbers is plotted and shown in figure 7(d). It is concluded from figure 7, the nanogenerator has shown high stability and durability similar to the reported literature [35–37].

4. Conclusion

In this work, hot plate-assisted hydrothermal growth of ZnO nanosheet networks is reported for the first time. A growth temperature of 85 °C and a growth duration of 4 h is optimum for uniform and dense ZnO nanosheets. XRD and TEM study confirms the crystallinity and purity of the ZnO nanosheet films. The nanogenerator is fabricated by placing ITO coated PET on the top of the ZnO nanosheets film. The switching polarity test and linear superposition of voltage tests confirms the generated voltage from nanogenerator. The proposed nanogenerator produced an open-circuit voltage and an instantaneous power of ∼220 mV and 65 nW. The proposed work demonstrated the ease of process, simplicity, and cost-effectiveness. Further, this nanogenerator performance can be improved with doping and composite ZnO films.

Acknowledgments

The authors are grateful to the funding agency SERB, DST, Govt. of India for kindly supporting the study reported in this paper, in the form of this project (ECR project No. # SERB/ECR/2016/000802)

The authors are grateful to the Center for Advanced Materials (CAM) and Center for Automation and Instrumentation (CAI) for the microscope facility and x-ray diffraction facility, National Institute of Technology, Warangal.

ORCID iDs

P Supraja https://orcid.org/0000-0001-5612-4035
Rakesh Kumar R https://orcid.org/0000-0003-4023-9051
Siju Mishra https://orcid.org/0000-0003-3774-4196
D Haranath https://orcid.org/0000-0002-7936-6165
P Ravi Sankar https://orcid.org/0000-0001-5652-0759
K Prakash https://orcid.org/0000-0001-9009-7325

References

[1] Anderson T R, Hawkins E and Jones P D 2016 CO_2, the greenhouse effect and global warming: from the pioneering work of arrhenius and callendar to today's earth system models *Endeavour* **40** 178–87
[2] Omer A M 2009 Energy use and environmental impacts: a general review *J. Renew. Sustain. Energy* **1** 053101
[3] Zhang C, Fan W, Wang S, Wang Q, Zhang Y and Dong K 2021 Recent progress of wearable piezoelectric nanogenerators *ACS Appl. Electron. Mater.* **3** 2449-2467
[4] Wang Z L and Song J 2006 Piezoelectric nanogenerators based on zinc oxide nanowire arrays *Science* **312** 242–6
[5] Hu Y, Lin L, Zhang Y and Wang Z L 2012 Replacing a battery by a nanogenerator with 20 V output *Adv. Mater* **24** 110–4
[6] Liu Z, Zhang S, Jin Y M, Ouyang H, Zou Y, Wang X X, Xie L X and Li Z 2017 Flexible piezoelectric nanogenerator in wearable self-powered active sensor for respiration and healthcare monitoring *Semicond. Sci. Technol.* **32** 64004

[7] Yu A, Song M, Zhang Y, Kou J, Zhai J and Lin Wang Z 2014 A self-powered AC magnetic sensor based on piezoelectric nanogenerator *Nanotechnology* **25** 455503
[8] Hu Y and Wang Z L 2014 Recent progress in piezoelectric nanogenerators as a sustainable power source in self-powered systems and active sensors *Nano Energy* **14** 3–14
[9] Leung S F, Ho K T, Kung P K, Hsiao V K S, Alshareef H N, Wang Z L and He J H 2018 A self-powered and flexible organometallic halide perovskite photodetector with very high detectivity *Adv. Mater.* **30** 1–8
[10] Wang Z L 2009 Ten years' venturing in ZnO nanostructures: from discovery to scientific understanding and to technology applications *Chinese Sci. Bull.* **54** 4021
[11] Gomez J L and Tigli O 2013 Zinc oxide nanostructures: from growth to application *J. Mater. Sci.* **48** 612–24
[12] Baruah S and Dutta J 2009 Hydrothermal growth of ZnO nanostructures *Sci. Technol. Adv. Mater.* **10** 13001
[13] Gerbreders V, Krasovska M, Sledevskis E, Gerbreders A, Mihailova I, Tamanis E and Ogurcovs A 2020 Hydrothermal synthesis of ZnO nanostructures with controllable morphology change *CrystEngComm* **22** 1346–58
[14] Kim K H, Kumar B, Lee K Y, Park H K, Lee J H, Lee H H, Jun H, Lee D and Kim S W 2013 Piezoelectric two-dimensional nanosheets/anionic layer heterojunction for efficient direct current power generation *Sci. Rep.* **3** 2017
[15] Ueno N, Yamamoto A, Uchida Y, Egashira Y and Nishiyama N 2012 Low-temperature hydrothermal synthesis of ZnO nanosheet using organic/inorganic composite as seed layer *Mater. Lett.* **86** 65–8
[16] Gaddam V, Kumar R R, Parmar M, Yaddanapudi G R K, Nayak M M and Rajanna K 2015 Morphology controlled synthesis of Al doped ZnO nanosheets on Al alloy substrate by low-temperature solution growth method *RSC Adv.* **5** 13519–24
[17] Kamruzzaman M and Zapien J A 2018 Effect of temperature, time, concentration, annealing, and substrates on ZnO nanorod arrays growth by hydrothermal process on hot plate *Crystallogr. Reports* **63** 456–71
[18] Yang R, Qin Y, Li C, Dai L and Wang Z L 2009 Characteristics of output voltage and current of integrated nanogenerators *Appl. Phys. Lett.* **94** 22905
[19] Il P K *et al* 2012 Flexible nanocomposite generator made of $BaTiO_3$ nanoparticles and graphitic carbons *Adv. Mater.* **24** 2999–3004
[20] Gupta M K, Lee J H, Lee K Y and Kim S W 2013 Two-dimensional vanadium-doped ZnO nanosheet-based flexible direct current nanogenerator *ACS Nano* **7** 8932–9
[21] Yu A, Li H, Tang H, Liu T, Jiang P and Wang Z L 2011 Vertically integrated nanogenerator based on ZnO nanowire arrays *Phys. status solidi - Rapid Res. Lett.* **5** 162–4
[22] Zhou Y, Liu W, Huang X, Zhang A, Zhang Y and Wang Z L 2016 Theoretical study on two-dimensional MoS_2 piezoelectric nanogenerators *Nano Res.* **9** 800–7
[23] Xu Q and Qin Y 2017 Theoretical study of enhancing the piezoelectric nanogenerator's output power by optimizing the external force's shape *APL Mater.* **5** 074101
[24] Lee H J, Sherrit S, Tosi L P, Walkemeyer P and Colonius T 2015 Piezoelectric energy harvesting in internal fluid flow *Sensors (Switzerland)* **15** 26039–62
[25] Nadaud K, Morini F, Dahiya A S, Justeau C, Boubenia S, Rajeev K P, Alquier D and Poulin-Vittrant G 2018 Double buffer circuit for the characterization of piezoelectric nanogenerators based on ZnO nanowires *Appl. Phys. Lett.* **112** 1–6
[26] Sultana A, Alam M M, Garain S, Sinha T K, Middya T R and Mandal D 2015 An effective electrical throughput from PANI supplement ZnS nanorods and PDMS-based flexible piezoelectric nanogenerator for power up portable electronic devices: an alternative of MWCNT filler *ACS Appl. Mater. Interfaces* **7** 19091–7
[27] Sensor S P, Li X, Lin Z, Cheng G, Wen X, Liu Y and Niu S 2014 3D fiber-based hybrid nanogenerator for energy harvesting and as a Self-Powered Pressure Sensor *ACS Nano* **8** 10674–81
[28] Rafique S, Kasi A K, Kasi J K, Aminullah, Bokhari M and Shakoor Z 2020 Fabrication of silver-doped zinc oxide nanorods piezoelectric nanogenerator on cotton fabric to utilize and optimize the charging system *Nanomater. Nanotechnol.* **10** 1–12
[29] Stassi S, Cauda V, Ottone C, Chiodoni A, Fabrizio C and Canavese G 2015 Flexible piezoelectric energy nanogenerator based on ZnO nanotubes hosted in a polycarbonate membrane *Nano Energy* **13** 474–81
[30] Ye S *et al* 2019 High-performance piezoelectric nanogenerator based on microstructured P(VDF-TrFE)/BNNTs composite for energy harvesting and radiation protection in space *Nano Energy* **60** 701–14
[31] Bird J 2014 *Electrical Circuit Theory and Technology* 5th ed.
[32] Park K *et al* 2014 Highly-effi cient *Flexible piezoelectric PZT Thin Film Nanogenerator on Plastic Substrates* Adv. Mater. **26** 2514–20
[33] Luo C, Hu S, Xia M, Li P, Hu J, Li G, Jiang H and Zhang W 2018 A flexible lead-free $BaTiO_3$/PDMS/C composite nanogenerator as a piezoelectric energy harvester *Energy Technol.* **6** 922–7
[34] Garain S, Jana S, Sinha T K and Mandal D 2016 Design of *in Situ* poled Ce3+-doped electrospun PVDF/graphene composite nanofibers for fabrication of nanopressure sensor and ultrasensitive acoustic nanogenerator *ACS Appl. Mater. Interfaces* **8** 4532–40
[35] Yu D, Zheng Z, Liu J, Xiao H, Huangfu G and Guo Y 2021 Superflexible and lead-free piezoelectric nanogenerator as a highly sensitive self-powered sensor for human motion monitoring *Nano-Micro Lett.* **13** 1–12
[36] Mokhtari F, Foroughi J, Zheng T, Cheng Z and Spinks G M 2019 Triaxial braided piezo fiber energy harvesters for self-powered wearable technologies *J. Mater. Chem. A* **7** 8245–57
[37] Kim S K, Bhatia R, Kim T H, Seol D, Kim J H, Kim H, Seung W, Kim Y, Lee Y H and Kim S W 2016 Directional dependent piezoelectric effect in CVD grown monolayer MoS_2 for flexible piezoelectric nanogenerators *Nano Energy* **22** 483–9